Journal of Engineering, Project, and Production Management
2026, 16(5), 2025-312

Real-Time Monitoring and Operation Optimization Strategies for Carbon Emissions of Large Urban Public Buildings

Yinghui Zou
Vice Dean, School of Civil Engineering, Liaodong University, Dandong,118003, China, E-mail: YinghuiZou18@outlook.com

Project Management
Received December 8, 2025; revised January 20, 2026; accepted July 7, 2026
Available online July 20, 2026

Abstract: Addressing the shortcomings of traditional static carbon accounting methods, such as low time resolution and a lack of carbon-oriented building operation strategies, this study proposes a real-time monitoring system and operation optimization strategy based on dynamic carbon footprint. A high-precision dynamic carbon accounting model is constructed, a multi-level monitoring system is developed, and an optimization model to minimize carbon costs is established. Experimental findings demonstrate that the dynamic accounting method can avoid a maximum carbon emission accounting bias of 4.80%. The optimization strategy achieves a 12.5% reduction in carbon emissions on peak carbon days, an 8.5% monthly reduction, and a cumulative reduction of 52.6 tons of CO_2 equivalent, while reducing total electricity costs by 2.1%. Building electricity consumption characteristics are significantly improved, with a 15.8% reduction in average daily peak carbon power and a 6.5% increase in load factor. In conclusion, this research provides a carbon management solution for large urban public buildings that combines environmental and economic benefits, and has significant practical value for promoting the low-carbon transformation of the building sector.

Keywords: Carbon accounting; dynamic carbon footprint; carbon emissions; carbon signal; building.

DOI 10.32738/JEPPM-2025-312

1. Introduction

In the context of intensifying global climate change and the continued advancement of the "dual carbon" goal, the building sector, as a significant contributor to energy use and carbon emissions (CEs), has made low-carbon transformation a crucial element in achieving sustainable development (Yang et al., 2023). Currently, CEs during the building operation phase account for a large share of society's total emissions. Among them, large public buildings, owing to their large scale, complex systems, and high energy intensity, have become a focus and a challenge for building CE reduction. In recent years, with the rapid development of technologies such as intelligent sensing and the Internet of Things, monitoring and energy-saving optimization of building energy consumption (EC) have made great progress. However, there are still severe challenges in the refined management of CEs.

To advance carbon management, many scholars have conducted research. Usman and Abdullah (2023) constructed an analytical evaluation model that can be used to analyze the characteristics of building EC and greenhouse gas emissions, to tackle the challenge that it is difficult to quantify the EC and CEs of buildings throughout their entire life cycle and that there is a lack of systematic tools for emission reduction strategies. Actual measurements were conducted on four teaching buildings and one library. The findings demonstrated that the energy intensity of three of the cases was as low as 80, 60, and 64 kWh/m²·year, respectively, indicating excellent practice. Yin and Zhao (2024) constructed an analytical framework to examine the impact of government regulation on the development of the green and intelligent building materials industry, aiming to address the insufficient motivation for the green transformation of the traditional building materials industry under the "dual carbon" target. Experimental simulation found that if the government implemented appropriate regulation on building materials enterprises, it could significantly incentivize enterprises to break through technical barriers, expand green production capacity, and help achieve CE reduction and sustainable development Kusi et al. (2025) proposed a building information model transformation scheme of “UAV imagery + 3D reconstruction + parametric modeling + EC simulation” to solve the problems of high building EC and large CEs. The experiment digitized a traditional building and calculated its EC. The findings demonstrated that the green renovation model could save 25% of energy and reduce carbon dioxide emissions by 46.8%. Hu et al. (2022) constructed a comprehensive China Building Energy and Emissions Model (CBEEM) to address the challenge posed by the lack of EC and CE data in the building sector, which leads to unclear "dual carbon" paths and difficulty in tracking progress. The model recalculated the national buildings into two major stages: construction and operation. In 2020, the EC of building operation was 1.06 billion Tonnes of Coal Equivalent (TCE). The EC of construction was 520 million TCE. The CE of operation was 2.2 billion t CO_2, and the CE of construction was 1.5 billion t CO_2.

Despite previous research achieving certain results, several limitations remain. First, most carbon accounting methods employ a fixed time scale, rendering it challenging to capture the dynamic changes in grid carbon intensity. Second, existing research often focuses on EC targets for operational optimization, lacking a systematic consideration of carbon costs and economics. Furthermore, existing research often disconnects monitoring and optimization processes, failing to establish a complete carbon management technology system. To manage these issues, this research introduces a comprehensive solution integrating dynamic carbon footprint accounting, real-time monitoring, and operational optimization, aiming to promote refined carbon management of large urban public buildings. Compared with the existing carbon sensing control research, the novelty of this paper is mainly reflected in the level of systematic integration and engineering application. Existing research has either focused on the theoretical analysis of the dynamic carbon signal of the power grid or been limited to the simulation and optimization of the building EC model. CE accounting, real-time monitoring and operation control are often regarded as independent links. This study builds a complete technical closed loop from short-time dynamic carbon sensing and minute-level EC monitoring to model-prediction-based rolling optimization, and realizes a seamless connection between data flow and control flow. Specifically, this study not only uses the dynamic marginal emission factor for high-precision accounting but also develops a deeply coupled real-time monitoring system and an optimal controller based on hybrid prediction. This approach transforms the innovative carbon signal theory into a deployable and verifiable engineering solution. A long-term empirical study conducted in a large-scale public building has verified its comprehensive efficiency in continuous emission reduction and grid coordination, making up for the lack of "perception decision control" chain disconnection in the current study.

2. Methods and Materials

2.1. Development of Dynamic Carbon Footprint Accounting Model and Real-Time Monitoring System

Accurate quantification and real-time perception of the dynamic changes in CEs during building operation are key to achieving refined carbon management of large public buildings in cities. Traditional static carbon accounting methods based on annual or monthly energy bills are unable to capture the high-frequency dynamic characteristics of carbon footprint driven by real-time fluctuations in grid carbon intensity, start-up and shutdown of building energy-consuming equipment and load changes, as well as the time-varying characteristics of external climate conditions (Jiang et al., 2022). This limitation seriously restricts the formulation and implementation of data-driven, real-time strategies for optimizing building operations. To tackle this problem, this research proposes developing a dynamic carbon footprint accounting model with high spatio-temporal resolution and an integrated real-time monitoring system based on it, thereby laying a solid data foundation for accurate assessment of building carbon performance and low-carbon optimization of operational strategies. The dynamic carbon footprint accounting model is shown in Fig. 1.

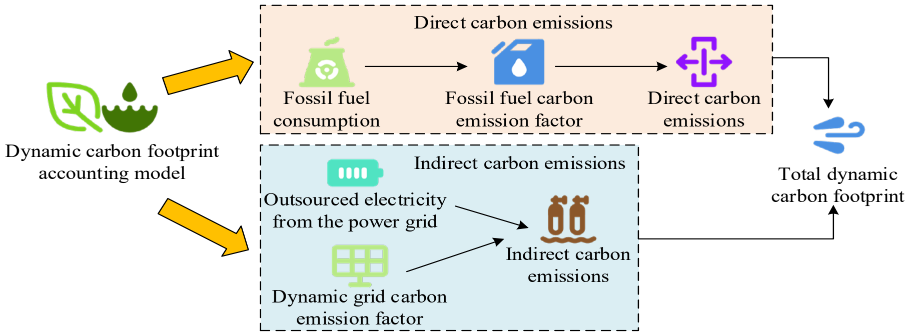

Fig. 1. Dynamic carbon footprint accounting model (icon source: https://iconpark.oceanengine.com/official)

In Fig. 1, the model follows the principle of defining the operational boundary in the life cycle assessment, focuses on CEs during the building operation phase, and deconstructs them into two categories: direct CEs and indirect CEs. At the same time, the model introduces a time dimension, which shifts CE accounting from long-term static statistics to hourly dynamic calculations, thereby enabling an accurate depiction of the instantaneous trajectory of the building's carbon footprint (Goswami et al., 2025). In this process, the total CEs of the building at any time t, calculated in carbon dioxide equivalent, can be expressed as Eq. (1).

$$CF_{total}(t) = CF_{direct}(t) + CF_{indirect}(t) \tag{1}$$

In Eq. (1), $CF_{total}(t)$represents the total dynamic carbon footprint, $CF_{indirect}(t)$represents the CEs implied by the building's consumption of purchased electricity at time t indirect dynamic CEs (Garimella et al., 2022). $CF_{direct}(t)$ represents the CEs generated by the building's direct combustion of fossil fuels at time t, direct dynamic CEs (Sun et al., 2022). The calculation of direct CEs relies on real-time monitoring of fuel consumption and fixed emission factors; the specific calculation method is given in Eq. (2).

$$CF_{direct}(t) = \sum_i [E_{fuel,i}(t) \times EF_{fuel,i}] \quad (2)$$

In Eq. (2), $E_{fuel,i}(t)$ is the real-time consumption of the ith type of fossil fuel at time t. The fossil fuel consumption. $EF_{fuel,i}$ represents the carbon dioxide equivalent emission corresponding to consuming one unit of the ith type of fossil fuel, i.e., the fossil fuel CE factor (Cheng and Hu, 2023). As for indirect CEs, since the key to its accounting lies in accurately characterizing the change law of grid CE intensity over time, the study adopts the concept of dynamic marginal emission factor to represent it, as presented in Eq. (3).

$$CF_{indirect}(t) = E_{electricity}(t) \times EF_{grid}(t) \quad (3)$$

In Eq. (3), $E_{electricity}(t)$ represents the total electricity that the building receives from the municipal power grid at time t, and $EF_{grid}(t)$ is the dynamic grid CE factor at time t. This factor is obtained through a programmatic interface with an external data source, as shown in Fig. 2.

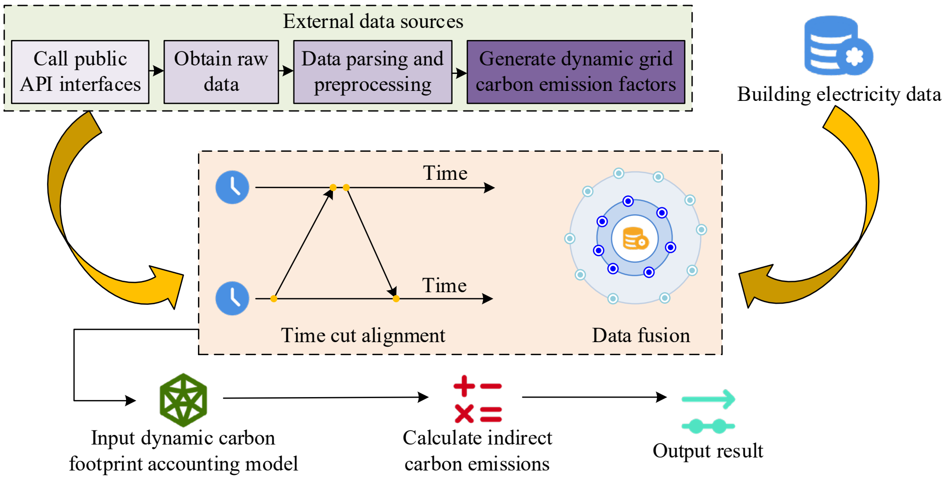

Fig. 2. Process for obtaining dynamic grid CE factors (icon source: https://iconpark.oceanengine.com/official)

As shown in Fig. 2, the study obtains carbon intensity data reflecting the current marginal emission level of the power system by calling the public application programming interface provided by the regional power grid operator at 1-hour time steps. After aligning this data with the building electricity consumption data with timestamps, it is input into the dynamic carbon footprint accounting model for calculation. The resulting indirect CE accounting can accurately reflect the carbon cost at the moment of electricity consumption (Guo et al., 2024; Liu et al., 2025). To ensure that the above theoretical model can be translated into a stable and reliable engineering application, the study also developed a multi-level, real-time building CE monitoring system.

At the physical sensing layer, the system integrates and extends the building's existing building automation system and energy metering architecture. Deploying and utilizing existing smart sensing devices at the building's energy inlets and key end-user energy systems enables automated, minute-level collection of various EC data across the entire building. At the data communication and aggregation layer, the system uses industry-standard communication protocols to construct a data acquisition network. Smart meters distributed throughout the system transmit the collected raw data packets to locally deployed edge computing gateways or directly to the central data server via fieldbus and industrial Ethernet, ensuring dependable, low-latency data transmission from the source to the aggregation point.

In the core data processing and computing layer, the system has a dedicated data processing engine (Wang and Zhong, 2023; Herth and Blok, 2023). This engine undertakes multiple tasks, the primary of which is to perform automated preprocessing and quality control of the input raw energy data stream. In this stage, the system uses an unsupervised machine learning algorithm based on isolated forests to detect outliers and identify and process noisy data caused by momentary sensor failures or communication interference, ensuring the reliability of the data stream. In addition, the engine is responsible for coordinating the fusion of internal and external data, scheduling a call to the external dynamic carbon signal API via a programmatic interface, and aligning and matching the acquired grid carbon intensity time series data with the internal EC data using timestamps. Finally, as the execution core of the accounting model, the engine also needs to load the static emission factor parameters stored in the database, drive the dynamic carbon footprint accounting formula to perform real-time calculation, generate the CE intensity sequence of the building as a whole, each sub-system and key equipment, and store all results in a structured time series database to provide a standardized data source for subsequent applications. In the application presentation layer, the system provides a web-based platform for user interaction and visualization. This platform presents multidimensional carbon information to building facility managers through a comprehensive dashboard. This level can transform abstract CE data into intuitive and actionable decision-making information, completing a full closed loop from data collection and processing to the final value presentation.

To ensure the reliability of the monitoring system and the effectiveness of the database, system performance and data quality were continuously evaluated throughout the entire research cycle. In the physical perception layer, 285 intelligent sensors were deployed in the system, which were specifically distributed as follows: 150 metering sensors for lighting and socket circuit, 95 sensors for the central air conditioning system (including chillers, pumps and air handling units), 15 sensors for the elevator system and 25 metering sensors for building total electricity, natural gas and regional cooling inlet. The data sampling frequency of all sensors was set to once per minute. During the entire 7-month research period, the system's comprehensive data acquisition success rate was 99.75%, with success rates of 99.78%, 99.70% and 99.68% for power consumption, natural gas and regional cooling data acquisition, respectively. Through automatic quality control by the data processing engine, the overall proportion of effective data across the entire cycle reached 99.05%, providing high-quality, continuous and stable data support for dynamic carbon footprint accounting and optimization analysis.

2.2. Building Operation Optimization Model Based on Dynamic Carbon Signals

While dynamic carbon footprint accounting models and real-time monitoring systems can accurately perceive and quantify building CEs, achieving carbon reduction requires translating this perception capability into effective control actions. Therefore, based on real-time feedback of dynamic carbon signals, this study further constructs a building operation optimization model oriented towards optimal carbon cost. This model aims to proactively respond to fluctuations in grid carbon intensity by adjusting the building's energy system operation strategy, thereby minimizing CEs during operation while ensuring indoor environmental comfort, as shown in Fig. 3.

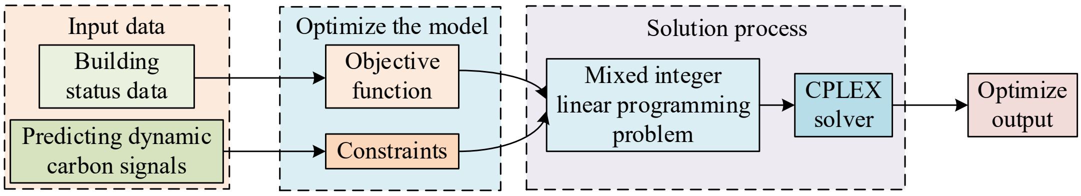

Fig. 3. Building operation optimization model

Fig. 3 shows the building operation optimization model. The core idea of this model is to regard the building's flexible load, especially the HVAC system, as a dispatchable virtual carbon sink resource (Pan et al., 2023). The model takes the minimum total CE cost in the next optimization cycle (24 hours) as the objective function, as shown in Eq. (4).

$$min\,J = \sum_{t=1}^{T}[EF_{grid}(t) \cdot P_{grid}(t) \cdot \Delta t] \tag{4}$$

In Eq. (4), $EF_{grid}(t)$ represents the total CE cost over the entire optimization period, Trepresents the total number of time periods within the optimization period, $EF_{grid}(t)$ represents the predicted grid CE factor for time period t obtained from the prediction model, $P_{grid}(t)$ represents the electrical power obtained by the building from the grid during time period t, and Δtrepresents the duration of each time step (Chen et al., 2024). The optimization of the objective function is achieved by adjusting the operating settings of the building's energy system, while also satisfying a series of strict physical and comfort constraints. These constraints collectively define the feasible region of the optimization. There are four types of constraints: indoor thermal comfort constraint, building thermodynamic constraint, system equipment performance constraint, and power grid interaction constraint. Among them, the indoor thermal comfort constraint requires that the indoor temperature of the building must be maintained within a range that is comfortable for the human body, which can be expressed as Eq. (5).

$$T_{setpoint,min} \leq T_{in}(t) \leq T_{setpoint,max} \tag{5}$$

In Eq. (5), $T_{in}(t)$ is the average indoor temperature over time period t, $T_{setpoint,min}$ and $T_{setpoint,max}$ are the lower and upper limits of the comfortable temperature (Fan et al., 2025). For building thermodynamic constraints, the indoor temperature variation can be determined by the thermal inertia of the building envelope and the output of the Heating, Ventilation and Air Conditioning (HVAC) system, as presented in Eq. (6).

$$C\frac{dT_{in}(t)}{dt} = \frac{T_{out}(t)-T_{in}(t)}{R} + Q_{internal}(t) - Q_{HVAC}(t) \tag{6}$$

In Eq. (6), C is the building's equivalent heat capacity, $R$is the building's equivalent thermal resistance, $T_{out}(t)$ is the outdoor temperature during time period t, $Q_{internal}(t)$ is the indoor heat gain, and $Q_{HVAC}(t)$ is the cooling/heating power of the HVAC system (Sarkar et al., 2024). The system equipment performance constraints require that the operating power of the HVAC host and other equipment be within the normal operating range, as shown in Eq. (7).

$$P_{HVAC,min} \leq P_{HVAC}(t) \leq P_{HVAC,max} \tag{7}$$

In Eq. (7), $P_{HVAC}(t)$ represents the electrical power of the HVAC host during time period t, and $P_{HVAC,min}$ and $P_{HVAC,max}$ represent the min and max power limits, respectively. The power grid interaction constraint requires that the power interaction between the building and the power grid be limited by the actual circuit capacity, as shown in Eq. (8).

$$0 \leq P_{grid}(t) \leq P_{grid,max} \tag{8}$$

In Eq. (8), $P_{grid,max}$ is the maximum allowable power at the grid connection point. Considering that the solution of this optimization model depends on the prediction of future dynamic carbon signals, a hybrid prediction method combining an autoregressive integral moving average model and a long short-term memory neural network is adopted, as shown in Fig. 4.

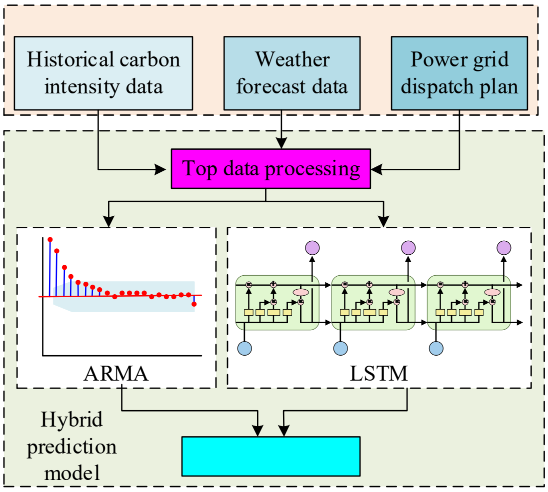

Fig. 4. Schematic diagram of the hybrid prediction method

Fig. 4 illustrates the hybrid prediction method. Based on historical carbon intensity data, weather forecasts, and power grid dispatch plans, a predicted sequence of power grid CE factors for the next 24 hours, with a step size of 1 hour, can be generated. After obtaining the predicted sequence, the optimization problem is transformed into a mixed-integer linear programming problem, which can then be efficiently solved using the CPLEX solver. The solver outputs a series of optimal equipment start-up and shutdown commands and setpoint adjustment strategies. Ultimately, this rolling optimization framework based on model predictive control enables buildings to transform from passive energy consumers into intelligent units capable of actively responding to power grid carbon signals and participating in system carbon regulation.

3. Results

3.1. Performance Analysis of Dynamic Carbon Monitoring System and Optimization Model

To confirm the efficacy of the dynamic carbon monitoring system and the operation optimization model, a large-scale commercial office building in a megacity in China's hot-summer, cold-winter climate zone was selected as the research object. The building's operating hours and personnel density followed typical office rules. The use peak was in the daytime on weekdays (Monday to Friday), and it was significantly reduced at night and on weekends. The HVAC system consisted of a centralized cooling station (chiller) and an air handling unit, and was connected to the regional cooling pipe network provided by municipal utilities. Under the benchmark scenario, the indoor temperature setting followed a fixed schedule strategy, with 26 ℃ for cooling in summer and 20 ℃ for heating in winter. The building had a total floor area of 85,000 square meters and included a central air conditioning system, lighting system, elevator system, and other office electrical equipment. The experimental monitoring period was the entire 2023 heating season (January 1st to January 31st), and the actual operating data during this period was used as the baseline scenario. The optimization model operated on the predicted 24-hour grid carbon intensity signal. A model predictive control framework was used for rolling optimization at 00:00 on each operating day to generate the optimal operating strategy for flexible loads such as the HVAC system. The experiment first evaluated the data acquisition and processing capabilities of the dynamic carbon monitoring system. The system used 285 smart sensors deployed at various energy inlets in the building to collect EC data for electricity, natural gas, and district cooling at a frequency of once per minute. The specific performance of the system during the one-week trial operation period (January 1st to January 7th, 2023) is shown in Fig. 5.

Fig. 5(a) shows the data acquisition success rate. During the one-week trial operation, the overall data acquisition success rate of the system was 99.81%. Specifically, the success rates for electricity consumption, natural gas, and district cooling data were 99.80%, 99.76%, and 99.86%, respectively, all remaining extremely high. Fig. 5(b) shows the proportion of abnormal data. The overall abnormal data rate identified by the system was 0.60%. Specifically, the abnormal data rates for electricity consumption, natural gas, and district cooling data were 0.62%, 0.59%, and 0.50%, respectively. Fig. 5(c) shows the proportion of final valid data. After automated preprocessing and quality control by the data engine, the overall valid data rate of the system's final output reached 99.21%. Specifically, the valid data rates for electricity consumption, natural gas, and district cooling data were 99.18%, 99.17%, and 99.36%, respectively. These results indicated that the overall data quality of the dynamic carbon monitoring system was good, providing a reliable basis for subsequent accurate accounting and optimization. Next, the experiment compared the dynamic carbon footprint accounting method with the traditional static method for the calculation of daily CEs over a typical week, as shown in Table 1.

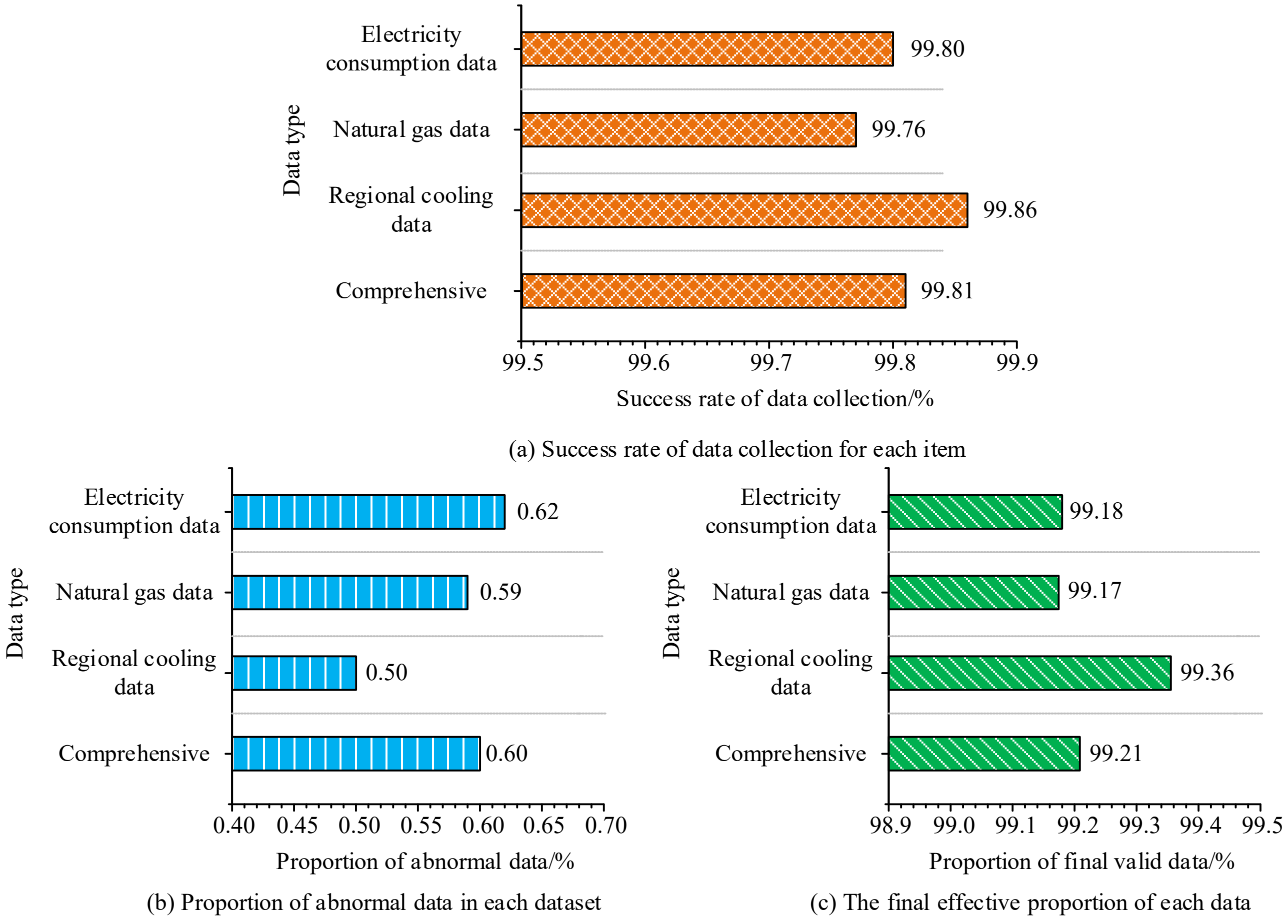

Fig. 5. Data quality assessment of the dynamic carbon monitoring system

Table 1. Comparison of CE results between dynamic and static accounting methods

Date	Total daily electricity consumption (kWh)	Average static factor ($kgCO_2e/kWh$)	Daily CE (Static)	Daily CE (Dynamic)	Absolute deviation	Relative deviation
2023/1/3	45,820	0.57	26.117	26.854	-0.737	-2.74%
2023/1/4	46,550	0.57	26.534	27.562	-1.028	-3.73%
2023/1/5	48,190	0.57	27.468	28.851	-1.383	-4.80%
2023/1/6	47,660	0.57	27.166	27.995	-0.829	-2.96%
2023/1/7	38,750	0.57	22.088	21.414	0.674	3.15%

As shown in Table 1, on weekdays with high grid carbon intensity (January 5th), static accounting underestimated actual CEs by 4.80%, whereas on weekends with low carbon intensity (January 7th), it overestimated them by 3.15%. This systematic bias indicated that traditional static accounting methods using fixed emission factors could not accurately reflect the true carbon cost of building operations, whereas dynamic accounting methods could capture temporal changes in CEs, providing a more reliable basis for carbon performance assessment and low-carbon optimization. Finally, the study quantitatively analyzed the carbon-reduction performance of the operational optimization model. The experiment compared the strategy generated by the optimization model (optimization scenario) with the actual building operation records (baseline scenario) in a simulated environment, and the results are shown in Fig. 6.

Fig. 6(a) shows the CEs under different scenarios, with January 10, 2023, as a normal working day, January 12, 2023, as a peak carbon day, and January 15, 2023, as a low carbon day. Under the baseline scenario, the CEs for these three days were 28,150 $kgCO_2e$, 29,880 $kgCO_2e$, and 20,540 $kgCO_2e$, respectively. Under the optimized scenario, the CEs for these three days were 25,890 $kgCO_2e$, 26,145 $kgCO_2e$, and 19,220 $kgCO_2e$, respectively. Based on these values, the difference between the two scenarios (i.e., the CE reduction) could be further calculated, yielding 2,260 $kgCO_2e$, 3,735 $kgCO_2e$, and

1,320 $kgCO_2e$, respectively. The resulting CE reduction rates were 8.0%, 12.5%, and 6.4%, respectively. Fig. 6(b) shows the total EC under different scenarios. Under the baseline scenario, the total EC for these three days was 48,200 kWh, 49,550 kWh, and 39,100 kWh, respectively. Under the optimized scenario, the total EC for these three days was 48,750 kWh, 51,430 kWh, and 39,050 kWh, respectively. Based on the difference between the two scenarios, the EC change rates for these three days could be calculated as +1.1%, +3.8%, and -0.1%, respectively. This result indicated that the optimized model could effectively identify and utilize the temporal differences in grid carbon intensity, maximizing CE reduction benefits at the lowest energy cost.

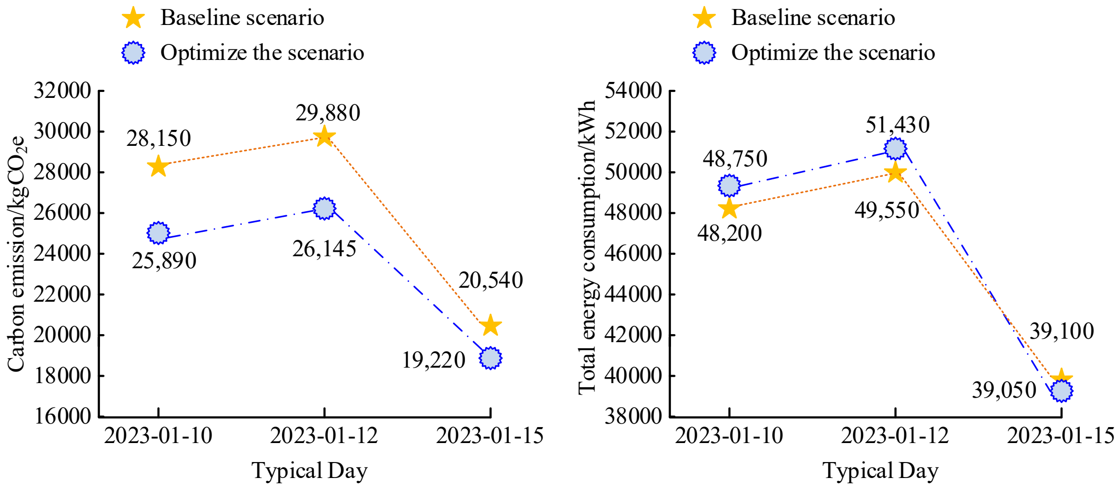

(a) Carbon emissions under different scenarios

(b) Total energy consumption in different scenarios

Fig. 6. Performance of the optimization model on a typical day

In addition, the experiment also evaluated the accuracy of the hybrid prediction model. The study used the historical data of hourly grid CE factors from January 1, 2021, to December 31, 2022, released by the grid operator in the region where the case building was located, and combined the dry bulb temperature and relative humidity data provided by the weather station in the same period as the external characteristics to form the training and verification data set. The training set and verification set were divided in an 8:2 ratio based on the time series. The key hyperparameters of the model were determined after a grid search and Optimization: the ARIMA order (P=2, d=1, q=2) was adopted; the LSTM part contained a hidden layer with 64 neurons, the dropout rate was set to 0.2, and the Adam optimizer was used for training. Table 2 shows the prediction error index of the model for the carbon intensity Series in the next 24 hours on the validation set.

Table 2. Performance metrics of the hybrid prediction model

Performance metric	Value
MAE	8.2 $kgCO_2e/MWh$
MAPE	5.70%
RMSE	10.5 $kgCO_2e/MWh$

The results in Table 2 showed that the hybrid model achieved high accuracy in predicting the power grid's carbon intensity over the next 24 hours, with a MAPE of less than 6%, providing a reliable, forward-looking carbon signal for subsequent rolling optimization decisions.

3.2. Case Studies of Optimization Strategies and Analysis of Emission Reduction Benefits

To thoroughly evaluate the potential and comprehensive benefits of building operation optimization strategies based on dynamic carbon signals in practical applications, this study selected the same case building mentioned above and applied the constructed model predictive control framework to its operation during the 2023 cooling season (July 1st - July 31st). The operational data after implementing the optimization strategy that month was defined as the “optimized scenario” and compared with the “baseline scenario,” simulated from historical operation logs using a fixed setpoint strategy. The core of the optimization strategy lies in guiding the building’s flexible loads (mainly the central cooling station) to avoid periods of high grid carbon intensity and prioritizing operation during low-carbon periods. The study first compared the two scenarios using a typical high-temperature workday (July 12th, 2023) as an example, as shown in Fig. 7.

Fig. 7(a) shows the chiller power results under different scenarios, and Fig. 7(b) shows the indoor temperature and average carbon grid intensity results for the same scenarios. During the peak carbon intensity period at midday (12:00-14:00), the optimized strategy increased the room temperature setpoint by appropriately pre-cooling the building and reducing chiller power to 35%-42%, thereby significantly reducing high-carbon electricity consumption. Conversely, during the early morning (06:00-08:00) and nighttime (22:00-24:00) periods with lower carbon intensity, the optimized strategy started the chiller earlier or operated it at higher power to store coolant for the building. Although the total daily electricity consumption was essentially the same as in the baseline scenario, the total CEs decreased by 10.7%, and the indoor temperature remained consistently within a comfortable range, thereby verifying the effectiveness and practicality of the strategy. To evaluate the macro-level benefits of the optimized strategy on a monthly scale, the key performance indicators for July were statistically analyzed and compared with the baseline scenario; the results are shown in Table 3.

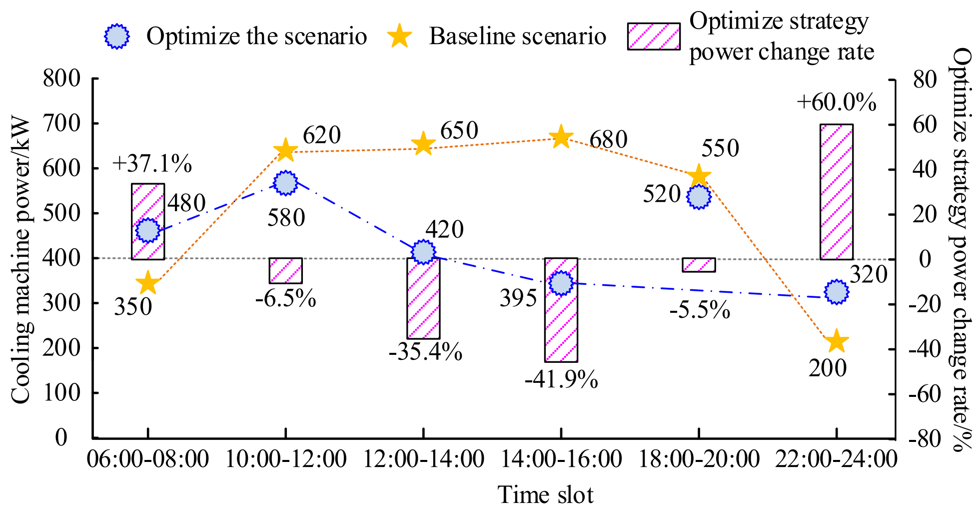

(a) Results of chiller power and its rate of change under different strategies

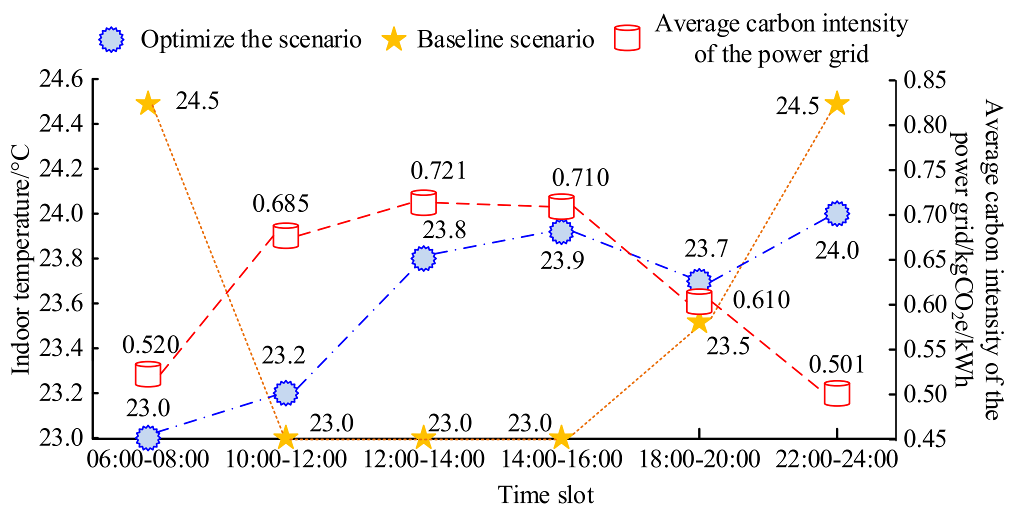

(b) Average grid carbon intensity and indoor temperature conditions

Fig. 7. Comparison of operating parameters between the optimized strategy and the baseline strategy

Table 3. Comparison of overall benefits between the optimized scenario and the baseline scenario for the whole month.

Performance indicator	Baseline scenario	Optimized scenario	Change amount	Change rate
Total CEs (tons CO_2e)	618.5	565.9	-52.6	-8.50%
Total electricity consumption (MWh)	1052.8	1065.4	12.6	1.20%
Average CE per unit area ($kgCO_2e/m^2$)	7.28	6.66	-0.62	-8.50%
Total electricity cost (CNY)	841,600	823,900	-17,700	-2.10%
Duration of indoor temperature exceeding standards (hours)	0	0	0	0

As shown in Table 3, the optimized strategy operated stably throughout the 31-day cooling season, achieving a reduction of 8.5% in total monthly CEs, amounting to a cumulative reduction of 52.6 tons of CO_2 equivalent. From an economic perspective, although total electricity consumption increased slightly (+1.2%) due to a slight decrease in system efficiency caused by partial load shifting, the total monthly electricity cost actually decreased by 2.1% because it effectively avoided electricity consumption during periods of high electricity prices. This indicated that the optimized strategy could achieve a win-win situation for both environmental and economic benefits. Finally, the impact of the optimized strategy on building electricity consumption characteristics was analyzed, and the results are shown in Table 4.

As shown in Table 4, the optimization strategy significantly improved the building's electricity consumption patterns and enhanced its low-carbon synergy with the power grid. Specifically, the building's average daily peak carbon power decreased by 15.8%. The building's average load factor increased by 6.5%, and the electricity consumption curve flattened. Furthermore, the proportion of electricity consumption during daytime peak hours decreased by 10.3%, while the proportion during nighttime off-peak hours increased by 14.3%. This load-shifting characteristic effectively promoted peak shaving and valley filling in the power grid.

Table 4. Impact of optimization strategies on building electricity consumption characteristics and grid coordination

Electricity characteristic indicator	Baseline scenario	Optimized scenario	Change amount	Change rate
Average daily maximum electrical power (kW)	1,850	1,750	-100	-5.40%
Average daily carbon peak power (kW)	1,840	1,549	-291	-15.80%
Average daily minimum electrical power (kW)	380	450	70	18.40%
Average load factor (%)	65.1	69.3	4.2	6.50%
Average daytime (peak hours) electricity consumption share	58%	52%	-6%	-10.30%
Average nighttime (off-peak hours) Electricity consumption share	42%	48%	6%	14.30%

To statistically verify the reliability of the emission-reduction effect of the optimization strategy and to further analyze the trade-off relationship among CE reduction, operating cost and thermal comfort, this study analyzed daily data over 31 days. First, a paired-samples t-test was conducted on the daily CEs for the optimized and baseline scenarios. The results showed that the difference between the two scenarios was highly statistically significant ($t=-15.32$, $p<0.001$), and the 95% confidence interval of the average daily CEs reduction was [-1.71, -1.50] tons of CO2e. In addition, the specific results of the multi-objective performance and trade-off analysis of the optimization strategy are shown in Table 5.

Table 5. Multi-objective performance and trade-off analysis of optimization strategy

Performance metric	Baseline scenario mean	Optimized scenario mean	Change amount	Change rate	*p*-value
Daily CEs (ton CO_2e)	19.95	18.25	-1.7	-8.50%	< 0.001
Daily Electricity Cost (CNY)	27,148	26,578	-570	-2.10%	0.023
Daily Indoor Temperature Exceedance Duration (hour)	0	0	0	0%	—
Daily Carbon Peak Power (kW)	1,840	1,549	-291	-15.80%	< 0.001

Table 5 presents a comprehensive overview of the optimization strategy's performance on the core objectives. The results showed that under the hard constraint of strictly maintaining indoor thermal comfort (the duration of temperature exceeding the standard was zero), the strategy simultaneously achieved significant reductions in CEs and electricity costs ($p<0.05$), with the CE reduction being highly significant ($p<0.001$). This revealed that, in this case, by using the dynamic carbon signal to guide load transfer, Pareto improvement can be achieved for the three-dimensional goal of "carbon cost comfort", rather than a trade-off, highlighting the advantages of the proposed method in collaborative optimization.

4. Discussion

This study proposed an operational optimization model that integrates a dynamic carbon footprint real-time monitoring system with model predictive control. Experimental results showed that the dynamic carbon accounting method could avoid a CE underestimation bias of up to 4.80% on typical working days. A CE reduction rate of 12.5% could be achieved on peak carbon days, with a cumulative monthly reduction of 52.6 tons of CO_2 equivalent (8.5%), while the total monthly electricity cost decreased by 2.1%. Furthermore, the optimization strategy reduced the building's average daily peak carbon power by 15.8% and increased the load factor by 6.5%, effectively promoting grid coordination. This research provided a different perspective on methodology and time scale. Peng et al. (2024) developed a BP neural network prediction model (GA-BP) based on genetic algorithm optimization to predict CEs in the construction industry at the provincial scale. By introducing the power correction coefficient and grey relational analysis, they achieved medium- and long-term scenario prediction of CEs in the construction industry in Sichuan Province. This study performed well in macro trend prediction (MAPE was 6.30%, R^2 was 0.853), but its time resolution was low, making it difficult to guide carbon optimization decisions in the daily operation of buildings. Xue et al. (2022) focused on the design of passive houses in frigid regions and developed an optimization framework integrating EC simulation, a neural network proxy model and a multi-objective genetic algorithm. They successfully achieved synergistic optimization of cost and CEs, on the premise that the life cycle cost remained essentially unchanged. This study provided a powerful tool for green building design, but its optimization object was static design parameters, which failed to cover the dynamic carbon signal response problem faced by buildings in operation.

In summary, this study optimized building operations by driving them using dynamic carbon signals, achieving a win-win for environmental and economic benefits while ensuring indoor environmental comfort. This provided a feasible technical approach for refined carbon management in large public buildings. However, the optimization model constructed in this study relied on deterministic predictions of the power grid's carbon intensity over the next 24 hours. The prediction uncertainty was mainly due to sudden changes in weather, fluctuations in renewable energy output, and changes in power grid dispatching strategy. The analysis showed that the CE reduction benefits of the model were sensitive to the prediction error: when the predicted peak time of carbon intensity deviated from the actual time by 1-2 hours, the CE reduction benefits of the day might be reduced by about 10% -15%. This revealed the problem that the optimization effect based on deterministic prediction might be limited when the prediction deviation was large. To enhance the ability of the system to deal with uncertainty, future research can be carried out from the following two aspects: first, stochastic model predictive control or robust optimization framework is used to incorporate the uncertainty of carbon intensity prediction into the optimization problem in the form of probability distribution or uncertainty set, so as to directly solve the robust strategy that can maintain good performance under uncertainty; The second is to further quantify and establish the sensitivity relationship between the prediction error and key performance indicators (such as CE reduction rate and cost savings), so as to provide the basis for more accurate prediction fault-tolerant mechanism or backup scheme for the system configuration. Through these approaches, it is expected to further improve the reliability and practicality of the dynamic carbon management strategy in a real, complex environment.

5. Conclusion

To address the challenges of precise CE management and operational optimization for large urban public buildings, this study developed a real-time monitoring system and an operational optimization model based on a dynamic carbon footprint. By sensing real-time fluctuations in grid carbon intensity and dynamically adjusting building EC behavior, effective reduction of CEs during building operation was achieved. Results showed that this model could significantly improve building carbon performance while ensuring indoor environmental comfort, and simultaneously promote low-carbon synergy between buildings and the power grid. Overall, this research provides a systematic technical framework and a practical pathway for refined, intelligent carbon management in large urban public buildings.

Based on the results of this study, the decision logic of construction facilities managers can change from "passive response" to "active prediction". Specifically, managers should extend the focus of decision-making from the traditional monthly electricity bill to the hourly dynamic carbon cost accounting; At the operational level, it is necessary to adjust the scheduling strategy of flexible loads such as air conditioning from a fixed period mode to a dynamic mode following the fluctuation of the carbon signal according to the carbon intensity prediction curve of the power grid. At the same time, managers should make full use of the equipment level carbon emission details provided by the real-time monitoring system to include the carbon performance into the daily operation and maintenance assessment indicators, so as to achieve the dual collaborative optimization of environmental objectives and economic costs under the premise of ensuring indoor comfort.

Funding

The research is supported by the 2024 Basic Scientific Research Project of Liaoning Provincial Department of Education: Research on Carbon Emission Control of Prefabricated Buildings under EPC Mode (Project No. LJ112411779025).

Institutional Review Board Statement

Not applicable.

Declaration of Artificial Intelligence (AI) Tools

The author used Grammarly Premium solely for language editing and readability improvement. The author reviewed and verified all content and takes full responsibility for the accuracy and integrity of the manuscript.

References

Chen, L., Hu, Y., Wang, R., Li, X., Chen, Z., Hua, J., Osman, A.I., Farghali, M., Huang, L., Li, J., and Dong, L. (2024). Green building practices to integrate renewable energy in the construction sector: A review. Environmental Chemistry Letters, 22(2), 751–784. doi: 10.1007/s10311-023-01675-2

Cheng, Z. and Hu, X. (2023). The effects of urbanization and urban sprawl on CO2 emissions in China. Environment, *Development and Sustainability,* 25(2), 1792–1808. doi: 10.1007/s10668-022-02123-x

Fan, T., Ren, Y., and Chapman, A. (2025). Unveiling the carbon neutrality pathways of compact cities: A simulation-bed scenario analysis from China. *Humanities and Social Sciences Communications*, 12(1), 55. doi: org/10.1057/s41599-025-05545-w

Garimella, S., Lockyear, K., Pharis, D., El Chawa, O., Hughes, M.T., and Kini, G. (2022). Realistic pathways to decarbonization of building energy systems. *Joule*, 6(5), 956–971. doi: 10.1016/j.joule.2022.03.001

Goswami, S. S., Mondal, S., Sarkar, S., Gupta, K. K., Sahoo, S. K. and Halder, R. (2025). Artificial intelligence-enabled supply chain management: Unlocking new opportunities and challenges. *Artificial Intelligence and Applications,* 3(1), 110–121. doi: 10.47852/bonviewAIA4202319

Guo, B., Feng, Y., and Hu, F. (2024). Have carbon emission trading pilot policy improved urban innovation capacity? Evidence from a quasi-natural experiment in China. *Environmental Science and Pollution Research,* 31(7), 10119–10132. doi: 10.1007/s11356-023-25699-x

Herth, A. and Blok, K. (2023). Quantifying universities' direct and indirect carbon emissions–the case of Delft University of Technology. *International Journal of Sustainability in Higher Education,* 24(9), 21–52. doi: 10.1108/IJSHE-04-2022-0121

Hu, S., Zhang, Y., Yang, Z., Yan, D., and Jiang, Y. (2022). Challenges and opportunities for carbon neutrality in China's building sector—Modelling and data. *Building Simulation,* 15(11), 1899–1921. doi: 10.1007/s12273-022-0912-1

Jiang, T., Li, S., Yu, Y., and Peng, Y. (2022). Energy-related carbon emissions and structural emissions reduction of China's construction industry: The perspective of input–output analysis. *Environmental Science and Pollution Research*, 29(26), 39515–39527. doi: 10.1007/s11356-021-17604-1

Kusi, E., Boateng, I., and Danso, H. (2025). Energy consumption and carbon emission of conventional and green buildings using building information modelling (BIM). *International Journal of Building Pathology and Adaptation*, 43(4), 826–854. doi: 10.1108/IJBPA-09-2023-0127

Liu, J., Jiang, M., Wang, Z., Wang, Z., Lu, M., Wang, L., and Zhang, X. (2025). A business model canvas for construction waste resource use under dual carbon targets. *International Journal of Construction Management*, 25(13), 1570–1582. doi: 10.1080/15623599.2024.2448141

Pan, H., Page, J., Shi, R., Cong, C., Cai, Z., Barthel, S., Thollander, P., Colding, J., and Kalantari, Z. (2023). Contribution of prioritized urban nature-based solutions allocation to carbon neutrality. *Nature Climate Change*, 13(8), 862–870.
doi: 10.1038/s41558-023-01737-x

Peng, S., Tan, J., and Ma, H. (2024). Carbon emission prediction of construction industry in Sichuan Province based on the GA-BP model. *Environmental Science and Pollution Research*, 31(16), 24567–24583. doi: 10.1007/s11356-024-32585-7

Sarkar, S., Naug, A., Luna, R., Guillen, A., Gundecha, V., Ghorbanpour, S., Mousavi, S., Markovikj, D. and Babu, A. R.(2024). Carbon footprint reduction for sustainable data centers in real-time. *Proceedings of the AAAI Conference on Artificial Intelligence,* 38(20), 22322–22330. doi: 10.1609/aaai.v38i20.30238

Sun, X., Zhang, H., Ahmad, M., and Xue, C. (2022). Analysis of influencing factors of carbon emissions in resource-based cities in the Yellow River basin under carbon neutrality target. *Environmental Science and Pollution Research,* 29(16), 23847–23860. doi: 10.1007/s11356-021-17386-6

Usman, A. M. and Abdullah, M. K. (2023). An assessment of building energy consumption characteristics using analytical energy and carbon footprint assessment model. *Green and Low-Carbon Economy*, 1(1), 28–40. doi: 10.47852 /bonviewGLCE3202545

Wang, X. and Zhong, M. (2023). Can digital economy reduce carbon emission intensity? Empirical evidence from China's smart city pilot policies. *Environmental Science and Pollution Research*, 30(18), 51749–51769. doi: 10.1007/s11356-023-26038-w

Xue, Q., Wang, Z., and Chen, Q. (2022). Multi-objective optimization of building design for life cycle cost and CO2 emissions: A case study of a low-energy residential building in a severe cold climate. *Building Simulation,* 15(1), 83–98. doi: 10.1007/s12273-021-0796-5

Yang, S., Yang, D., Shi, W., Deng, C., Chen, C., and Feng, S. (2023). Global evaluation of carbon neutrality and peak carbon dioxide emissions: Current challenges and future outlook. *Environmental Science and Pollution Research,* 30(34), 81725–81744. doi: 10.1007/s11356-022-19764-0

Yin, S. and Zhao, Y. (2024). An agent-based evolutionary system model of the transformation from building material industry (BMI) to green intelligent BMI under supply chain management. *Humanities and Social Sciences Communications*, 11(1), Article 55. doi: 10.1057/s41599-024-02988-5

Yinghui Zou is an Associate Professor at the School of Civil Engineering, Liaodong University. She graduated from Tianjin Institute of Light Industry in 1998, majoring in Mechanical Design and Manufacturing, and was awarded a Bachelor of Engineering degree. She obtained a second Bachelor of Engineering degree in Industrial Engineering from Northeastern University in 2001 and a Master of Economics from Liaoning Normal University in 2007. Currently, she serves as Vice Dean of the School of Civil Engineering, Liaodong University. She has published more than 20 academic papers and has presided over or participated in more than 20 scientific research projects. Her research Interests include digital engineering management, building energy monitoring and engineering carbon emission accounting.